

Recent AEM Case Study Examples Using a Full Waveform Time-Domain System for Near-Surface Applications*

Jean M. Legault¹, Alexander Prikhodko¹, Timothy Eadie¹, Greg Oldenborger², Vincenzo Sapia³, Andrea Viezzoli⁴, Erwan Gloaguen⁵, Bruce D. Smith⁶, and Melvyn E. Best⁷

Search and Discovery Article #41509 (2014)

Posted December 29, 2014

*Adapted from extended abstract prepared in conjunction with presentation at CSPG/CSEG/CWLS GeoConvention 2013, (Integration: Geoscience engineering Partnership) Calgary TELUS Convention Centre & ERCB Core Research Centre, Calgary, AB, Canada, 6-12 May 2013, Datapages/CSPG © 2014

¹Geotech Ltd., Aurora, Ontario, Canada (jean@geotech.ca)

²Geological Survey of Canada -Natural Resources Canada, Ottawa, Ontario, Canada

³National Institute of Geophysics and Volcanology (INGV), Rome, Italy

⁴Aarhus Geophysics, Aarhus, Denmark

⁵National Institute of Scientific Research (INRS), Quebec, QC, Canada

⁶USGS Crustal Geophysics and Geochemistry Science Center, Denver, CO, USA

⁷Bemex Consulting International, Victoria, B.C., Canada

Abstract

Early time or high frequency airborne electromagnetic data (AEM) are desirable for shallow sounding or mapping of resistive areas but this poses difficulties due to a variety of issues, such as system bandwidth, system calibration and parasitic loop capacitance. In an effort to address this issue, a continued system design strategy, aimed at improving its early-channel VTEM data, has achieved fully calibrated, quantitative measurements closer to the transmitter current turn-off, while maintaining reasonably optimal deep penetration characteristics. The new design implementation, known as “Full Waveform” VTEM was previously described by Legault et al. (2012). This paper presents some case-study examples of the Full Waveform VTEM helicopter time-domain EM system for near-surface applications.

Introduction

The Full Waveform (Legault et al., 2012) design implementation of the VTEM (versatile time-domain electromagnetic; Witherly et al., 2004) helicopter system is designed to achieve fully calibrated time-domain EM decays, particularly in early times (<100us), for better near-surface mapping than was previously possible with earlier VTEM helicopter system, while still maintaining its late-channel data quality for deeper penetration. The Full Waveform technology consists of a combination of 1) streamed half-cycle recording of transmitter and receiver waveform data, as well as 2) continuous system calibration corrections, 3) parasitic-noise and transmitter-drift corrections, and 4) ideal-waveform-deconvolution corrections, according to the method described by Macnae and Baron-Hay (2010). The latter three corrections are applied in a separate post-processing step (Legault et al., 2012).

Results of the Full Waveform VTEM surveys over these areas have led to improved accuracy of transient data at earlier times than previously achieved - as early as ~20 μ s after the current turn-off (versus ~100 μ s for standard VTEM) and as late as ~10 ms (channels 4-47). These, in turn, have also led to improvements in the model space that include better definition of the surficial layering and shallow structure, which appear to be in good agreement with known geology, based on case-study results.

Theory and Methodology

Deconvolution of airborne AEM to step response was first proposed by Annan (1986) for the "Prospect" fixed-wing system, which evolved into the Spectrum AEM system, and was later implemented in the Saltmap and Tempest AEM systems (Lane et al, 2000). The Full Waveform VTEM is the first commercial helicopter EM system to adopt waveform deconvolution (Legault et al., 2012; Macnae, 2012).

The sensor calibration procedure uses the measured calibration waveform for correction of half-cycle waveforms acquired on a survey flight. The half-cycle waveforms of each channel are corrected to obtain the waveforms that would be recorded if the time-domain responses of all the channels, including the reference channel, were from the same Gaussian-like, "ideal" response that is defined by its bandwidth.

A streamed current monitor and streamed receiver data are used for the continuous system response correction, as well as the transmitter drift and parasitic noise corrections, and ideal waveform deconvolution. The deconvolution procedure corrects, in frequency domain, one complete period for linear system imperfections including transmitter current drift through the following operation:

$$R(t) \Leftrightarrow R(\omega) = \frac{C_0(\omega) B(\omega)}{C(\omega) H_0(\omega)} W(\omega)$$

Where **R(t)** is the desired response (corresponding to **R(ω)** in frequency domain), **C** is the instantaneous current monitor and **C₀** the averaged high altitude reference current monitor measurement, **B** the instantaneous survey data and **H₀** the averaged high-altitude data respectively. **W(ω)** is an ideal waveform for which the response is desired (Macnae and Baron-Hay, 2010).

The VTEM survey results are initially processed using standard methods, with the system calibration correction and the parasitic-noise/transmitter-drift/ideal-waveform-deconvolution corrections applied in a separate post-processing step using the full-waveform data. The usable early time dBz/dt data following the system response correction and ideal waveform deconvolution typically improves from ~100usec to ~20usec after the end of current turn-off (Legault et al., 2012).

Examples

To test the full waveform VTEM system implementation, the Spiritwood Valley was chosen as a test area based on the availability of previous airborne and ground EM, electrical and seismic, borehole geophysical and well-log data from the study of a shallow freshwater aquifer by the Geological Survey of Canada (Oldenborger et al., 2010, 2011 and 2012). The Spiritwood Valley is a 10-15km wide, 100-150m deep,

northwest-southeast trending, buried bedrock valley that extends between Killarney and Cartwright ([Figure 1](#)) and extends 500km from Manitoba, across North Dakota and into South Dakota.

The valley lies within a till plain with little topographic relief but has been defined by a series of borehole transects and seismic reflection data collected north of Killarney. The stratigraphy within the valley is variable but includes a basal, shaly sand and gravel, and overlying clay-rich and silty till units. However, the sand and gravel is only found in incised valleys, making for a valley-within-valley morphology. The underlying bedrock is conductive, fractured siliceous shale. According to borehole resistivity log results, the simplified electrical section consists of three main units: 1) till (40-50 Ω -m), 2) sand and gravel (70-200 Ω -m) and 3) shale (5-50 Ω -m). The high resistivity of the sand and gravel makes it a marker unit for incised valleys that are groundwater targets, as shown in the precious helicopter TEM results in [Figure 1b](#) (Oldenborger et al., 2012).

To illustrate the differences and effects of Full Waveform data over regular VTEM, [Figure 2](#) presents Airbeo (Raiche, 1998) 1D layered-earth inversions for both data sets for a representative sounding along the northern line ([Figure 1](#)) over the incised valley aquifer where borehole Kilcart #8 is situated. In addition to borehole data, reflection seismic (S2007) and ground electrical tomography (ERI) results ([Figure 3](#)) provide good controls on the layering (Oldenborger et al., 2010). As shown, using the same initial models, the 1D inversion estimates using Full Waveform data ([Figure 2a](#)) with better calibrated early times ($>18 \mu\text{s}$) more closely resemble the known geology – as compared to those from regular VTEM data ([Figure 2b](#)) with later ($>96 \mu\text{s}$) uncalibrated early-time, whose layering in the upper 30 metres as well as the deeper geoelectrical information (i.e., overestimated resistivity for layer 3) are inaccurate.

[Figure 3a](#) shows an example of inverted resistivity models for ERI data acquired at the northern end of the survey area, and compares them to the 3C seismic reflection data for line S2007. The resistivity results show the relatively higher resistivities associated with the deepest part of the valley, suggesting that these sediments are potential aquifer targets. Synthetic modeling of the inversion results shows that the channel anomaly is consistent with erosion of both a supra-bedrock layer (till) and bedrock. The results indicate that ERI provides superior spatial resolution and compare very favourably with the seismic results (Oldenborger et al., 2012).

[Figure 3b](#) compares the same 3C seismic and ERI results against 1D spatially constrained inversion (SCI; Viezzoli et al., 2008) of the Full Waveform VTEM data across the northern survey line. The SCI inversions used an apriori forcing the near surface layers to be resistive, as per the ERI and the known geology. The improvements include better definition of the layering, including the surficial unsaturated till layer (unresolved using standard/non-full waveform VTEM data) and also a more compact resistive anomaly associated with the buried valley aquifer that is in better agreement with previous seismic and resistivity results.

Other ground and airborne case study comparisons from the St-Lawrence lowlands near St-Hyacinthe in the Montérégie region of Quebec, the Timiskaming kimberlite fields near New Liskeard in northeastern Ontario and the Nebraska Sandhills near the Crescent Lakes National Wildlife Refuge will illustrate near-surface resistivity mapping with the Full Waveform System. A similar case study will be presented from the Horn River Basin of northeastern British-Columbia using standard VTEM and 3D reflection seismic data ([Figure 4](#)).

Conclusions

Results of the Full Waveform VTEM surveys over the Spiritwood Valley aquifer and other near-surface geological case-studies have shown how improvements in quantitative data at earlier times – from approximately 96 μ s to as early as 18 μ s after the current turn-off and as late as 9.977 ms - have led to improvements in the model space that include better definition of the surficial layering and shallow structure that are in good agreement with the known geology.

Acknowledgements

The authors gratefully acknowledge the assistance of Geotech, NRCAN-GSC, USGS, INRS, Stornoway Diamond Corp., and Arcis Seismic Solutions.

References Cited

Annan, A. P., 1986, Development of the PROSPECT 1 airborne electromagnetic system: in G. Palacky, (ed), Airborne resistivity mapping, Geological Survey of Canada Paper 86-22, p. 63-70.

Lane, R., A. Green, C. Golding, M. Owers, P. Pik, C. Plunkett, D. Sattel, and B. Thorn, 2000, An example of 3D conductivity mapping using the TEMPEST airborne electromagnetic system: Exploration Geophysics, v. 31, p. 162-172.

Legault, J.M., A. Prikhodko, D.J. Dodds, J.C. Macnae, and G.A. Oldenborger, 2012, Results of recent VTEM helicopter system development testing over the Spiritwood Valley aquifer, Manitoba: 25TH SAGEEP Symposium on the Application of Geophysics to Engineering and Environmental Problems, EEGS, Expanded Abstract, 17 p.

Macnae, J., 2012, Broadband airborne electromagnetics: An update: a paper presented at KEGS-DMEC Geophysical Symposium 2012, Exploration '07 plus 5, A half decade of mineral exploration developments, 4 p.

Macnae, J., and S. Baron-Hay, 2010, Reprocessing strategy to obtain quantitative early-time data from historic VTEM surveys: 21ST International Geophysical Conference & Exhibition, ASEG Extended abstract, 5 p.

Oldenborger, G.A., A.J.-M. Pugin, M.J. Hinton, S.E. Pullan, H.A.J. Russell, and D.R. Sharpe, 2010, Airborne time-domain electromagnetic data for mapping and characterization of the Spiritwood Valley aquifer, Manitoba, Canada: Geological Survey of Canada, Current Research 2010-11, 13 p.

Oldenborger, G.A., A.J.-M. Pugin, and S.E. Pullan, 2011, Buried valley imaging using 3-C seismic reflection, electrical resistivity and AEM surveys: GeoHydro 2011: Joint meeting of the Canadian Quaternary Association and the Canadian Chapter of the International Association of Hydrogeologists, Expanded Abstract, 6 p.

Oldenborger, G., A.J.-M. Pugin, and S.E. Pullan, 2012, Airborne Time - Domain Electromagnetics for Three - Dimensional Mapping and Characterization of the Spiritwood Valley Aquifer: 25TH SAGEEP Symposium on the Application of Geophysics to Engineering and Environmental Problems, EEGS, Expanded Abstract, 5 p.

Raiche, A., 1998, Modelling the time-domain response of AEM systems: Exploration Geophysics, v. 29, p. 103–106.

Viezzoli A, A.V. Christiansen, E. Auken and K. Sørensen, 2008, Quasi-3D modeling of airborne TEM data by spatially constrained inversion: Geophysics, v. 73, p. F105–F113.

Witherly, K., R. Irvine, and E.B. Morrison, 2004, The Geotech VTEM time domain helicopter EM system: SEG Expanded Abstracts, v. 23, p. 1217-1221.

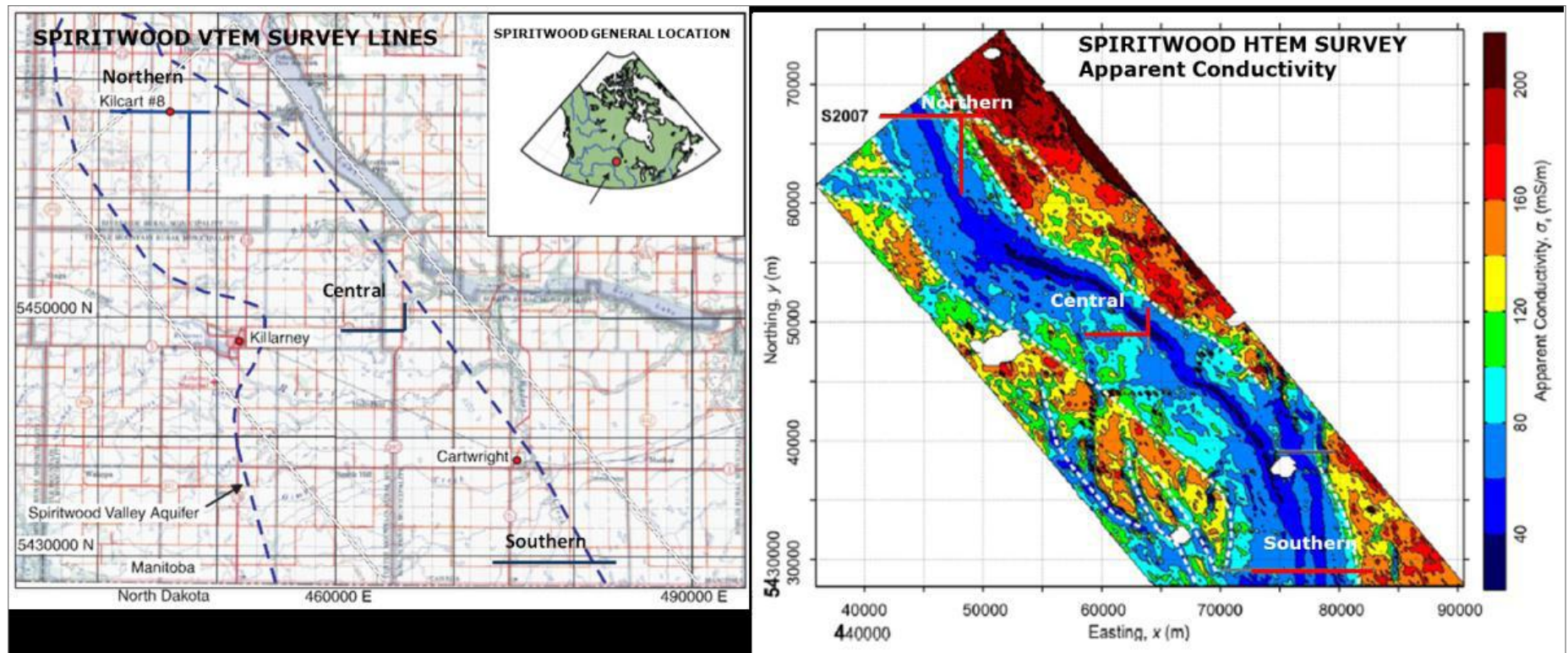


Figure 1. a) Spiritwood Valley location, aquifer outline (blue dash) from geologic mapping and 2011 VTEM test lines (blue solid), and b) Apparent conductivity and aquifer outline (white dash) from 2009 HTEM survey (modified after Oldenborger et al., 2012).

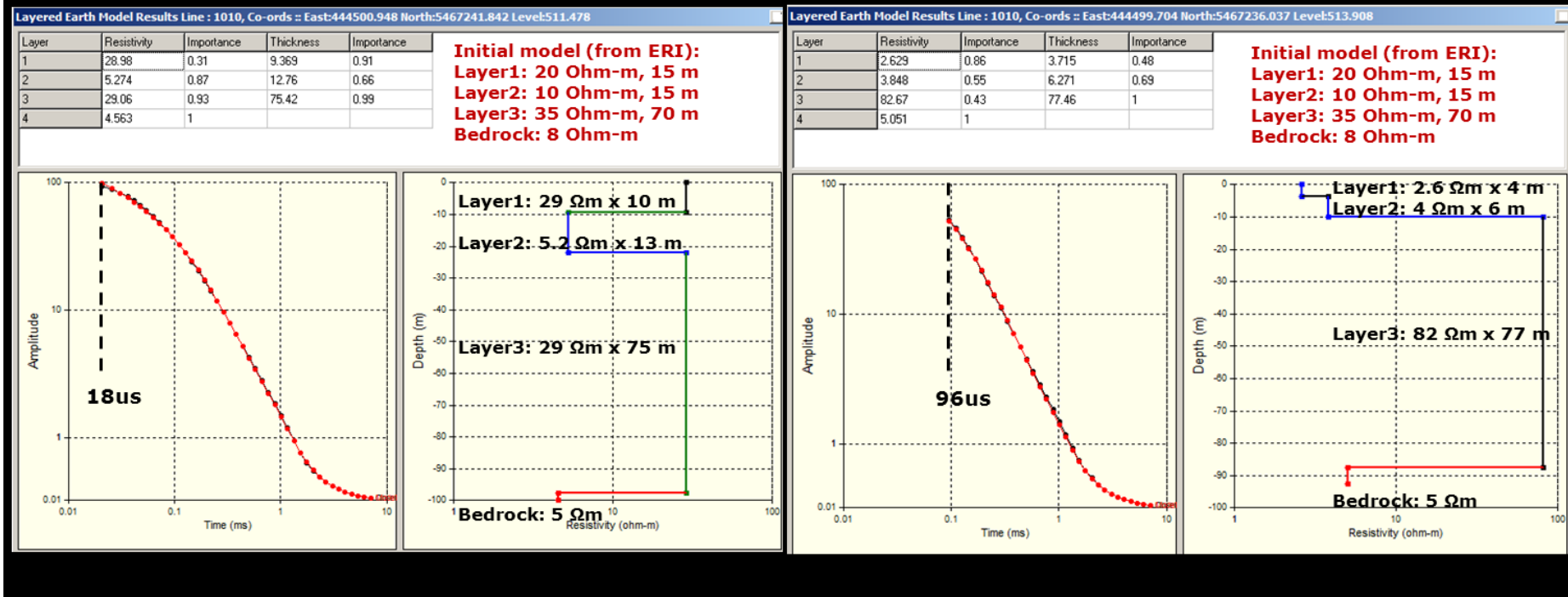
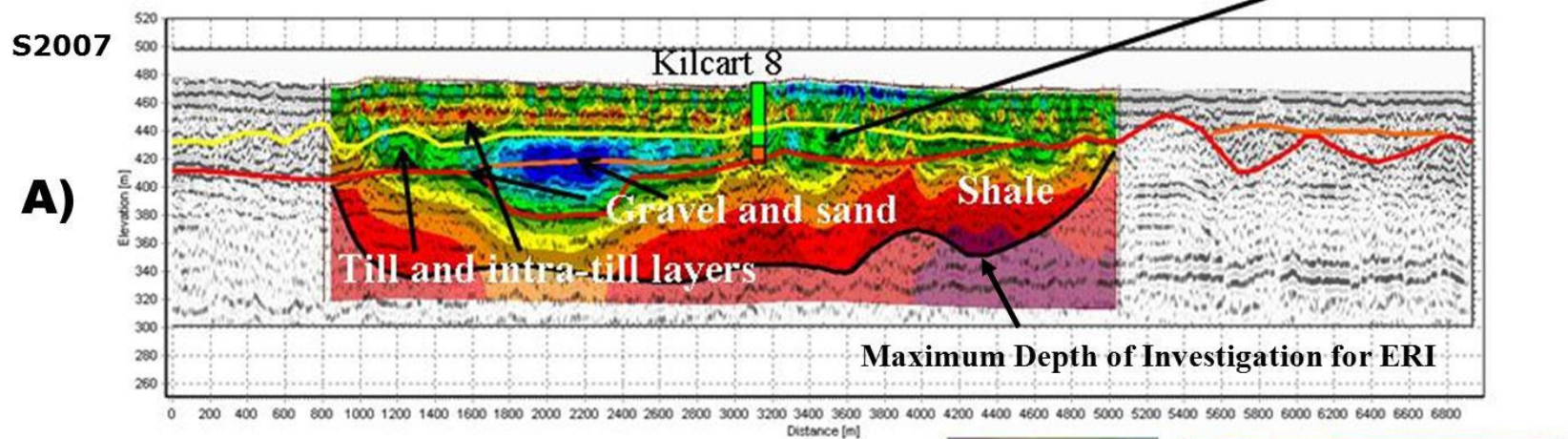


Figure 2. VTEM 1D inversions for northern profile (S2007) from a) Full Waveform and b) Regular data.

Electrical Resistivity Imaging (ERI) vs. 3C Seismic

Shale reflection from seismic



ERI vs. VTEM Spatially Constrained 1D Inversion (SCI)

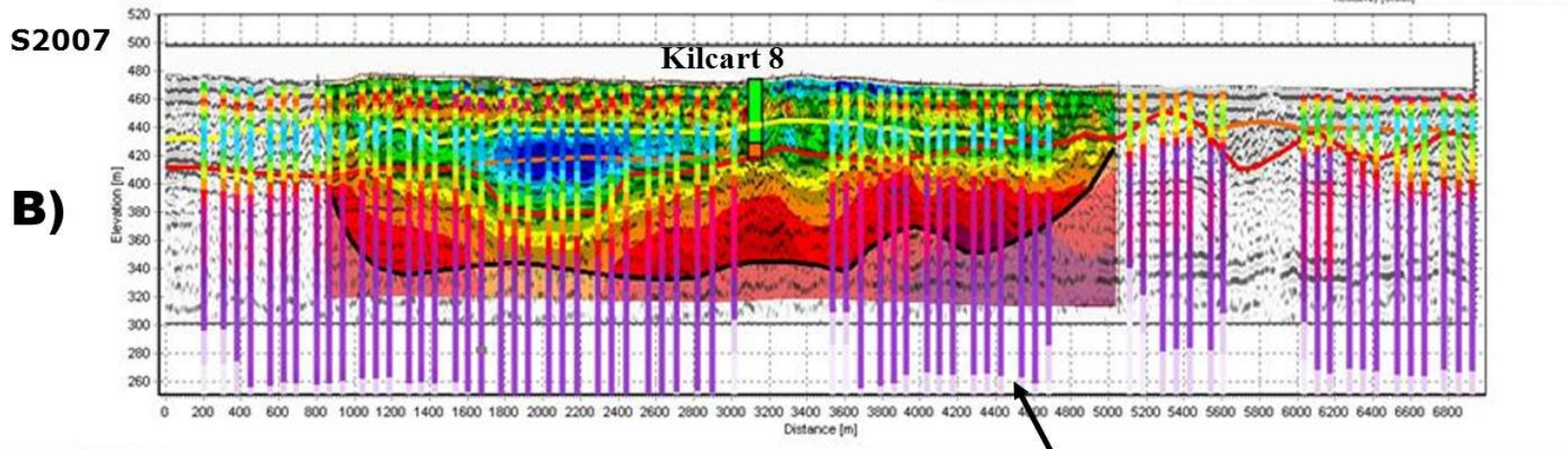


Figure 3. Profile S2007 a) ERI model overlain on interpreted seismic section. Interpreted gravel surface is orange, bedrock surface is red, and gravel-sand layer is yellow. The solid black line indicates the ERI depth of investigation. b) VTEM SCI layered-earth resistivity models overlain on interpreted seismic and ERI sections.

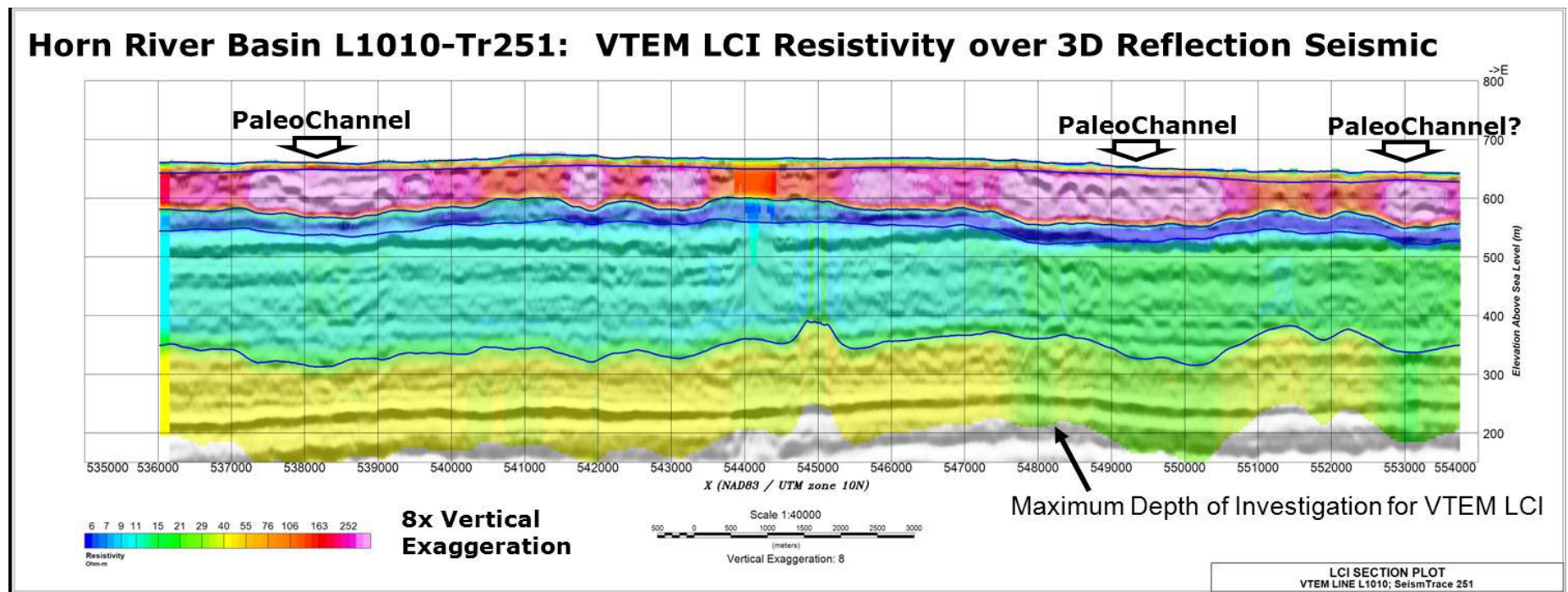


Figure 4. Horn River Basin a) Upper 400 m of the depth migrated 3D seismic section (line 1010) with VTEM laterally-constrained inversion (LCI) overlain in colour, showing potential paleochannels.